Article type : Special Issue Research Article

Reactive Oxygen Species-mediated Degradation of Antidiabetic Compounds: Cytotoxic Implications of Their Photodegradation Products†

Cecilia Challier[1*], Sergio Laurella[3], Patricia Allegretti[3], Carola Sabini[2], Liliana Sabini[2], Norman A. García[1], Alicia Biasutti[1], Susana Criado[1*]

[1] Departamento de Química, Universidad Nacional de Río Cuarto, (5800) Río Cuarto, Argentina

[2] Departamento de Microbiología, Universidad Nacional de Río Cuarto, (5800) Río Cuarto, Argentina

[3] Facultad de Ciencias Químicas, Universidad Nacional de La Plata, (4198) La Plata, Argentina

Corresponding authors' emails: scriado@exa.unrc.edu.ar (Susana Criado), cchallier@exa.unrc.edu.ar (Cecilia Challier)

†This article is part of a Special Issue dedicated to Dr. Norman "Andi" García.

ABSTRACT

Reactive Oxygen Species (ROS) have been described in their double physiological function, helping in the maintenance of health as well as contributing to oxidative stress. Diabetes mellitus is a chronical disease nearly related to oxidative stress, whose treatment (in type II variant) consists in the

administration of antidiabetic compounds (Andb) such as Gliclazide (Gli) and Glipizide (Glip). In this context, since Andb may be exposed to high ROS concentrations in diabetic patients, we have studied the potential ROS-mediated degradation of Gli and Glip through photosensitized processes, in the presence of Riboflavin (Rf) vitamin. We found that singlet oxygen ($O_2(^1\Delta_g)$) participated in the Rf-sensitized photodegradation of both Andb, and also superoxide radical anion in the case of Gli. Two principal products derived from $O_2(^1\Delta_g)$-mediated degradation of Gli were identified and their chemical structures characterized, through HPLC-Mass spectrometry. $O_2(^1\Delta_g)$-mediated degradation products and their toxicity was assayed on Vero cell line. These studies demonstrated that neither Gli nor its photoproducts caused cytotoxic effect under the experimental conditions assayed.
Our results show strong evidences of ROS-mediated Andb degradation, which may involve the reduction or loss of their therapeutic action, as well as potential cytotoxicity derived from their oxidation products.

INTRODUCTION

During the last years, several studies have demonstrated that reactive oxygen species, ROS (singlet oxygen ($O_2(^1\Delta_g)$), superoxide radical anion, hydroxyl radical and hydrogen peroxide) present in the organism may have a double function. On the one hand, the important role that ROS have in the maintenance of health, through their participation in several defenses and metabolic processes such as chemical signaling under hypoxia, vascular diameter maintenance, immune response, among others has been reported (1-3). On the other hand, ROS can be deleterious under some conditions due to their high reactive character (4-6). There are different factors that generate a progressive accumulation of ROS in cells, scenario known as oxidative stress. In these conditions, ROS levels are high enough to induce serious damaging processes. In fact, several investigations have demonstrated the near connection between oxidative stress and the development and complications of different diseases such as diabetes *mellitus* (type I and type II), cancer (7), insulin resistance (8), cardiovascular disease (9), and atherosclerosis (10).

Particularly, diabetes mellitus deserves a special attention due to the fact that this disease affects an important percentage of the worldwide population (11). Diabetes is characterized by disrupted insulin secretion and sensitivity, leading to high blood glucose levels. Strong evidence indicates that high glucose concentrations may induce a cascade of biochemical processes that increase ROS concentrations (12), which also produce damage in pancreatic beta cells (13).

Among all therapies indicated for diabetes type II, the use of antidiabetic drugs (Andb) such as sulphonylurea family has been found the most efficient treatment. These compounds act by stimulating insulin secretion through ATP-sensitive potassium channels closure in pancreatic beta cells (14).

In this context, due to the existence of an inherent oxidative stress condition associated to diabetes disease, and the possibility that Andb may be exposed to high ROS concentration, it would be of great interest to investigate the possible ROS-mediated degradation of Andb, such as Gliclazide (Gli) and Glipizide (Glip). The importance of these studies lies in the fact that these compounds may lose their therapeutic action, as well as in the potential toxicity of products derived from their interaction with ROS.

In this contribution, the degradation of Gli and Glip under oxidative stress conditions was investigated in the presence of the vitamin Riboflavin (Rf), a natural dye able to produce different ROS through mechanism type II ($O_2(^1\Delta_g)$) and/or mechanism type I (radical species). Particularly, in order to investigate the $O_2(^1\Delta_g)$-mediated degradation products, the sensitizer Perinaphtenone (PN) was employed as an exclusive $O_2(^1\Delta_g)$-generator. The characterization of these products was determined through HPLC-Mass spectrometry experiments. Furthermore, in order to evaluate the eventual toxicity of Gli in the presence of $O_2(^1\Delta_g)$, cytotoxicity assays using Vero cell line were performed. This cell line was selected because it is a model of primate cells that resemble human cells. Therefore, the toxic effects that a drug and/or their metabolic products can exert on the cellular system can be related (extrapoled) with those that could have on the human (15,16,17).

MATERIALS AND METHODS

Materials. Gliclazide (Gli), Glipizide (Glip), Riboflavin (Rf), Perinaphtenone (PN), sodium azide (NaN_3), catalase from bovine liver (CAT), superoxide dismutase (SOD), glutamine, gentamicin sulphate, neutral red and NaOH were purchased from Sigma-Aldrich-Argentina. Eagle´s minimum essential medium (EMEM) was provided by GIBCO, fetal calf serum (FCS) from Natocor and thioglycollate from Difco. NaCl, KCl, Na_2HPO_4-$2H_2O$, KH_2PO_4 and $NaCO_3H$ were purchased from Anedra. CH_3OH (HPLC quality) was obtained from Sintorgan.

In sensitized-photodegradation experiments, due to low Andb solubility in aqueous solutions, methanol was employed as a co-solvent (10%) in 0.1 M phosphate buffer solution (pH 7.4). In cytotoxicity studies, DMSO was employed as co-solvent at final concentrations less than 1%.

Vero cell line, from African green monkey (*Cercopithecus aethiops*) kidney cells ATCC CCL-81, was employed for cytotoxicity experiments. This cell line was acquired from Asociación Banco Argentino de Células (ABAC), Pergamino, Buenos Aires, Argentina.

Stationary photolysis. Stationary photolysis experiments were carried out in a home-made photolizer, as was previously described elsewhere (18,19). It comprises a quartz halogen lamp (150 W) as the excitation source. Light is passed through a water filter and then focused into a sample cell. The light was filtered using an appropriate cut-off filter, in order to ensure that it was only absorbed by the sensitizer. Samples were irradiated employing a quartz cuvette of 1 cm path length as the sample cell. In oxygen uptake experiments, the light was focused into a hermetically sealed reaction cell (50 mL) containing a specific oxygen electrode (Orion 97-08). All samples were continuously stirred.

Ground-state absorption spectra were carried out in a double beam spectrophotometer Shimadzu 2401.

Stationary and time-resolved fluorescence. In order to investigate the interaction between Andb and the electronically excited singlet state of Rf (^{1}Rf*), stationary and time-resolved fluorescence experiments were performed.

Fluorescence emission spectra of Rf in the absence and in the presence of Andb were recorded in a Spex Fluoromax spectrofluorometer.

Rf fluorescence lifetimes were determined with time-correlated single photon counting technique (SPC) employing an Edinburgh FL9000CD instrument.

In stationary and time-resolved experiments, 445 nm and 524 nm were used as excitation and emission wavelengths, respectively. All determinations were performed at 25 ± 1°C and quartz cells of 1.0 cm path-length were used.

The potential ^{1}Rf*-Andb interaction was determined through time-resolved experiments. The values of the rate constants for the quenching of ^{1}Rf* by Andb (^1k_q) were graphically determined through Stern-Volmer treatment (Eq. 1)

$$^1\tau_0 / {}^1\tau = 1 + {}^1k_q \, {}^1\tau_0 \, [\text{Andb}] \qquad (1)$$

where $^1\tau_0$ and $^1\tau$ are Rf fluorescence lifetimes in the absence and in the presence of Andb, respectively.

Laser flash photolysis experiments. In order to study the interaction between the electronically excited triplet state of Rf (^{3}Rf*) and Andb, the rate constant for the quenching of ^{3}Rf* by Andb (^3k_q) and the transient absorption spectra of Rf, in the absence and in the presence of Andb, were determined.

These experiments were performed through laser flash photolysis technique. The equipment has been previously described elsewhere (19). Briefly, it is provided with a frequency-doubled output of a Nd:YAG laser system (Spectron) at 355 nm as the excitation source and a 150 W xenon lamp as analyzing light. The detection system comprised a photon technology international monochromator and a red-extended photomultiplier (Hamamatsu R666).The output of the detector was coupled to a digital oscilloscope (Hewlett-Packard 54504A) and to a personal computer for processing the signal.

All determinations were performed in argon-saturated buffered solutions (pH 7.4, methanol 10%) in order to avoid ^{3}Rf*-$O_2(^3\Sigma_g^-)$ quenching (Scheme 2, process [7]) (20). The experiments were carried out at low Rf concentration (*ca* 0.01 mM) and low enough laser energy with the aim of preventing triplet-triplet annihilation or self-quenching undesirable effects.

The transient absorption spectra of Rf and Rf/Andb were acquired at different delay times in order to visualize the formation of Rf transient species and their deactivation by Andb and/or the formation of new transient species derived from the interaction between excited-Rf and Andb.

The interaction between ^{3}Rf*-Andb was quantified through Stern-Volmer analysis (Eq. 2),

$$^3\tau_0 / {}^3\tau = 1 + {}^3k_q \, {}^3\tau_0 \, [\text{Andb}] \qquad (2)$$

where $^3\tau_0$ and $^3\tau$ are ^{3}Rf* lifetimes in the absence and in the presence of Andb, respectively; and ^3k_q is the rate constant for the quenching of ^{3}Rf* by Andb. Transient lifetimes were determined from ^{3}Rf* first-order decays observed at 670 nm, where the potential interferences of other transient species remain insignificant (21).

Participation of ROS in the Rf-sensitized photodegradation of Andb. In order to investigate the possible participation of ROS in the Rf-sensitized photodegradation of Andb, oxygen uptake experiments in the absence and in the presence of specific additives with ROS-scavenging abilities were made using the home-made photolyzer previously described. In this case, light at λ <361 nm was filtered using a cut-off filter in order to ensure that it was only absorbed by Rf. The compounds as ROS inhibitors employed were NaN_3 for singlet oxygen ($O_2(^1\Delta_g)$), CAT for hydrogen peroxide (H_2O_2) and SOD for superoxide anion radical ($O_2^{\bullet-}$).

From initial slopes of oxygen uptake plots in the absence (v_0) and in the presence of the mentioned inhibitors (v_{Inh}), the values of relative rates of oxygen consumption (v_r) were calculated ($v_r = v_{Inh} / v_0$).

HPLC-Mass characterization of the photoproducts derived from the $O_2(^1\Delta_g)$-mediated photodegradation of Andb. With the aim to identify the photoproducts derived from the reaction between $O_2(^1\Delta_g)$ and Andb, HPLC-Mass Spectrometry experiments were performed. In these experiments the sensitizer, Perinaphtenone (PN) was employed as an exclusive $O_2(^1\Delta_g)$ generator (22).

Stationary aerobic photolysis of solutions containing Andb and PN were carried out in the home-made photolyzer previously described. In this case, light at λ <320 nm was filtered using an appropriate cut-off filter. Samples, continuously oxygenated and stirred, were irradiated for 60 min.

HPLC-Mass Spectrometry analyses were made in a Thermo Scientific Accela equipment, provided with a quaternary pump, a spectrometric ion trap (Thermo Scientific LQT XL) and auto-sample system. The HPLC separation of the analytes was performed on a reverse phase C_{18} column (150 mm x 2.1 mm x 5 μm), under isocratic mode employing water: methanol (9:1 v/v) and 0.2 mM ammonium acetate as mobile phase. The flow rate was 0.2 mL/min and the injection volume was 10 μL. Samples were ionized using electrospray ionization (ESI) and detected in a positive mode. All determinations were made at room temperature.

Analysis of cytotoxicity of Gli in the presence of $O_2(^1\Delta_g)$. With the purpose of investigating the potential cytotoxicity of Gli in the presence of $O_2(^1\Delta_g)$, Vero cell line was used as an *in vitro* experimental model. Cells cultures were propagated in growth medium (GM), which comprises EMEM supplemented with 10% FCS, 30 μg/mL glutamine and 50 μg/mL gentamycin, at pH 7.2-7.4. Cells were seeded at 37°C in 96-wells culture plates until monolayer formation ($3x10^4$ cells/well). Afterwards, cells were washed and incubated with the samples under study for 48 h. Untreated cells were used as a control. In all experiments, cells were treated with different volumes of stock solutions Gli/PN as well as volumes of maintenance medium (MM), to reach a final volume of 200 μL/well. MM has the same composition as GM, but supplemented with 2% FCS. Due to low Andb solubility in water solutions, DMSO was used as co-solvent at non-cytotoxic concentration (less than 1%) (23).

Maximum non-cytotoxic concentration (MNCC) was determined microscopically, through direct samples observation after 48 h of incubation.

Vero cells viability was measured by Neutral Red Uptake assay (NRU) (24,25). After the incubation period with samples, Vero cells were washed with 200 μL of PBS buffer/well and 150 μL of Neutral Red dye solution (30 μg/mL dissolved in MEM) was added. Cells were incubated at 37°C for 3 h and washed thrice with PBS buffer. Neutral Red within viable cells was released by extraction with acetic acid, ethanol and water solution (1:50:49). Cultures were shaken for 20 min and absorbance values were determined at 540 nm (Neutral Red maximum absorbance) in a Labsystems Multiskan MS plate reader. Relative cell viability (RCV) was determined from the following equation:

$$RCV = A_{540nm} \text{ treated cells} / A_{540nm} \text{ untreated cells} \quad (3)$$

From plots of RCV vs. concentrations of studied compounds, the CC_{50} parameter can be graphically determined. CC_{50} is defined as the concentration of the compounds at which the relative cell viability attains 50%.

The results were statistically analyzed with the program GraphPad Prism 5. Standard deviation was calculated from three independent repetitions.

RESULTS AND DISCUSSION

Andb-Rf sensitized photodegradation.

Results presented in this section will be interpreted and discussed in terms of Scheme 2.

Scheme 2 shows potential kinetic pathways in a general sensitized process.

The incident light promotes the ground-state sensitizer, S, to its electronically excited singlet state, $^1S^*$, (process [1]) which through intersystem crossing process yields the electronically excited triplet state species $^3S^*$ (process [4]). An energy transfer process from $^3S^*$ to ground oxygen ($O_2(^3\Sigma_g^-)$) dissolved in the solution may produce singlet oxygen, $O_2(^1\Delta_g)$ (process [7]), which may decay by either collision with solvent molecules (process [9]) or by physical (process [10]) or chemical (process [11]) interaction with Andb. $^3S^*$ may interact with Andb through an electron transfer process to produce the semioxided $Andb^{+\bullet}$ and the semireduced $S^{-\bullet}$ species (process [8]). The radical $S^{-\bullet}$, in the presence of $O_2(^3\Sigma_g^-)$, may produce a cascade of processes that yield different ROS.

UV-Vis spectra of oxygenated solutions containing 1 x 10^{-4} M Gli / Rf ($A_{445\ nm}$~0.5), evaluated as a function of time of irradiation, showed spectral modifications in typical absorption zones of Andb (250-300 nm) as well as Rf (400-500 nm), as can be seen in Fig. 1. Same results were found in the case of Glip (Fig. 2, insert). In parallel, oxygen consumption was observed for both Andb (Fig. 1, insert).

These results yielded strong evidence of the interaction between Andb and the electronically excited states of Rf and/or different ROS generated from these states.

With the aim to investigate the potential interaction between the electronically excited singlet state of Rf ($^1Rf^*$) and Andb, stationary and time-resolved fluorescence experiments were performed. Rf emission spectrum is in good agreement with the reported one in previous researches (26). Results showed that Rf fluorescence emission intensity and $^1Rf^*$ lifetimes values ($^1\tau$) decrease under increasing concentrations of Gli. However, Rf emission spectrum shape did not change. Meanwhile, it seems that Glip did not affect the fluorescence emission nor $^1\tau$ (for 7.5 x10^{-3} M Glip as the highest concentration assayed). Stern-Volmer plot obtained from time-resolved fluorescence experiments is shown in Fig. 2. ^1k_q values, graphically determined from Fig. 2, are displayed in Table 1. These results demonstrated that only Gli interacts with $^1Rf^*$ under the experimental conditions assayed. However,

considering Gli concentrations employed in photooxidation experiments ([Gli] ~10^{-4} M) and the value of Rf fluorescence lifetime (27,28) in the absence of Gli ($^1\tau_0$ = 4.9 ns), the ^{1}Rf*-Gli interaction may be considered negligible.

In order to study the eventual interaction between the electronically excited triplet state of Rf (^{3}Rf*) and Andb, the UV-V spectrum of anaerobically irradiated Rf solutions was determined in the absence and in the presence of Andb. In the absence of Andb, the sensitizer showed a decrease in typical absorbance at 445 nm after irradiation. However, a smaller decrease in the absorbance of Rf was observed in the presence of Gli (Fig. 3, insert). These results suggest a possible interaction between Gli and ^{3}Rf* since Rf-photodegradation is known (20,29) to occur anaerobically from ^{3}Rf*. Similar results were obtained in the presence of Glip.

The eventual interaction between ^{3}Rf* and Andb was evaluated through laser flash photolysis technique (Materials and Methods) in argon-bubbled buffered solutions (pH 7.4, methanol 10%). Results showed a decrease in $^3\tau$ in the presence of Gli or Glip, which confirms an interaction between ^{3}Rf* and both Andb. Stern-Volmer plots of $1/^3\tau$ *vs.* [Andb] (Fig. 3, main) yielded the bimolecular rate constant values, ^3k_q, shown in Table 1.

In order to investigate the nature of the ^{3}Rf*-Andb interaction, transient spectrum of 0.01 M Rf was performed in the absence and in the presence of Andb ($5x10^{-4}$ M) in argon-saturated buffered solutions (pH 7.4, methanol 10%). Rf transient spectrum obtained 2 μs after the laser pulse in the absence of Andb is in good agreement with what was previously reported for Rf transient species (30). In the presence of Andb, the Rf transient spectrum obtained 20 μs after the laser pulse, showed a decrease over the range of 600-750 nm. (Fig. 4, main).

By comparing the transient spectrum in the absence of Andb (2 μs after the laser pulse), and the spectrum (20 μs after the laser pulse, normalized at 670 nm) in the presence of Andb (Fig. 4, insert), the appearance of a new band over 500-600 nm was observed. The latter can be attributed to the absorbance of the neutral radical of Rf ($RfH^{\bullet}$), which has already been reported by other authors (30). This radical is produced (Scheme 2, process [13]) from the protonation of $Rf^{\bullet -}$, generated in process [8]. It is known that the bimolecular decay of $RfH^{\bullet}$ yields Rf and fully reduced Rf (RfH_2) (31). The last species, in the presence of $O_2(^3\Sigma_g^-)$, may trigger several chain-events that yield different ROS, which may finally interact with Andb (Scheme 2).

With the aim of studying the participation of different ROS in Rf-sensitized photodegradation of Andb, oxygen uptakes experiments were performed through stationary irradiation of oxygenated buffered solutions of Andb in the absence and in the presence of specific ROS inhibitors: superoxide dismutase (SOD), catalase (CAT) and sodium azide (NaN_3). In previous studies (32-35), the use of these inhibitors has been reported as a helpful resource to confirm or discard the participation of $O_2(^1\Delta_g)$, H_2O_2 and $O_2^{\bullet -}$ in an oxidative degradation. SOD dismutates $O_2^{\bullet -}$ through reaction (a), Scheme 3, while CAT decomposes H_2O_2 as can be seen in reaction (b), Scheme 3. It is known that NaN_3 physically deactivates the species $O_2(^1\Delta_g)$, as shown in reaction (c), with a rate constant of $k_q = 3x10^8\ M^{-1}\ s^{-1}$ in water (33).

Fig. 5 shows oxygen consumption by Andb in the absence and in the presence of the mentioned ROS inhibitors. From the initial slopes of these plots, v_r values were calculated as described in the Materials and Methods section. These values were obtained as an average of three independent experiments (Table 2).

As can be seen in Table 2, the decrease in v_r values in the presence of NaN_3 for both Andb confirms the participation of $O_2(^1\Delta_g)$ in the Rf-sensitized photodegradation of Gli and Glip. In the case of Gli, an increment in v_r values in presence of SOD can be observed. This result may be explained in terms

of reactions showed in Scheme 2 and in Scheme 3. Formation of $O_2^{\bullet-}$ requires one $O_2(^3\Sigma_g^-)$ molecule (process [20], Scheme 2), meanwhile, in the presence of SOD the deactivation of two $O_2^{\bullet-}$ molecule yields only one $O_2(^3\Sigma_g^-)$ molecule (process (a), Scheme 3). This oxygen net balance may explain the increase in oxygen uptake relative rate observed in presence of SOD. This evidence is in agreement with previous research which have reported that this enzyme can either inhibit or stimulate the $O_2^{\bullet-}$ -mediated oxidation of different substrates (21,30,36,37).

Furthermore, no changes in oxygen uptakes were observed in the presence of CAT, indicating that the species H_2O_2 is not reactive against Gli. In case of Glip, under an experimental error of 10%, any changes in oxygen uptakes are observed neither in the presence of SOD nor in the presence of CAT. This evidence demonstrates that neither H_2O_2 nor $O_2^{\bullet-}$ interacts with Glip. Previous results suggest that Rf-sensitized photodegradation of Gli may occur via $O_2(^1\Delta_g)$ and $O_2^{\bullet-}$. In other words, the degradation of Gli may proceed through the combinations of type I and type II mechanisms. The occurrence of one pathway or the other will depend on the competition that will have oxygen (process [7], Scheme 2) or Gli (process [8], Scheme 2) by ^{3}Rf*. In this sense, it is well known that the value of k_{ET} (process [7], Scheme 2) represents 1/9 of the value of k_{diff} ($7x10^8$ $M^{-1}s^{-1}$) (38) and that ^3k_q yielded a value of $9.9x10^8$ $M^{-1}s^{-1}$ (value for Gli, process [8], Scheme 2). Taking into account these rate constants values and the experimental conditions ([Andb] = $5x10^{-4}$ M and $[O_2(^3\Sigma_g^-)] = 2x10^{-4}$ M) it could be settled that the rate of ^{3}Rf*-deactivation by Gli (process [8], Scheme 2) is only 3.5 times higher than the rate of deactivation by $O_2(^3\Sigma_g^-)$ (process [7], Scheme 2). Therefore, it can be said that both processes would be competitive.

In case of Glip, our results suggest that its photodegradation may occur only via $O_2(^1\Delta_g)$ (type II mechanism).

$O_2(^1\Delta_g)$-mediated degradation of Andb: products identification and cytotoxicity assays

As was demonstrated, $O_2(^1\Delta_g)$ participates in the Rf-sensitized photodegradation of both Andb. In previous studies the specific $O_2(^1\Delta_g)$-mediated degradation of Gli and Glip was investigated, employing the artificial dye PN as $O_2(^1\Delta_g)$-sensitizer (39). From these studies, it was observed that the value of the rate constant of the overall $O_2(^1\Delta_g)$ deactivation ($k_t = k_q + k_r$, which accounts for the physical, k_q, and reactive, k_r, contribution to the overall deactivation, respectively) is greater for Gli than for Glip. These results suggest that Gli is more effective than Glip in $O_2(^1\Delta_g)$ deactivation. Furthermore, from reactive contribution evaluated through relative oxygen consumption rates (v_r), it can be noticed that Gli seems to be more reactive than Glip (39). Therefore, based on the greater reactivity observed between $O_2(^1\Delta_g)$ and Gli, and with the aim of complete previous investigations, an HPLC-Mass Spectrometry study of the products derived from this reaction was performed in this contribution. The samples were analyzed before and after 60 min of irradiation, using PN as the sensitizer. Results are summarized in Table 3.

Chromatographic analysis of the sample without irradiation showed a peak observed at 11.9 min, whose Mass Spectrometry analysis indicated the major contribution of the following ionic species in the positive ion mass spectrum: Gli molecular ion $[M+H]^+$ with m/z=324 uma, derived from protonation at the N-ring position in Gli and Gli molecular ion bound to potassium cation $[M+K]^+$ with m/z= 362 uma. The presence of a dimer of Gli produced by intermolecular hydrogen bond was also observed.

Sample irradiated during 60 min yielded the same chromatographic peak observed at 11.9 min with the same Mass Spectrometry analysis as the sample without irradiation. As can be noticed in Table 3, two new chromatographic peaks that did not appear in the sample before irradiation were found at t_R= 3.9 min and t_R= 13.2 min. Through fragmentation analysis, possible chemical structures for these compounds may be suggested as shown in Table 3 (photoproducts 1 and 2).

The participation of $O_2(^1\Delta_g)$ in the photodegradation of Gli, represents a very interesting subject of study. In this sense, it would be of great importance to analyze the potential cytotoxicity of Gli in the presence of $O_2(^1\Delta_g)$, since both $O_2(^1\Delta_g)$ and Gli can share cellular environments in diabetic patients. In order to contribute to this aspect, *in vitro* cytotoxicity studies were performed.

Vero Cells were treated with aliquots of buffered solutions of Gli (1617 μg/mL, pH 7.4, DMSO at a final concentration less than 1%) in the presence of PN (less than 9.9 μg/mL) without irradiation and after 45 and 75 min of irradiation. As a complementary assay, PN cytotoxicity was evaluated under the experimental conditions. These studies demonstrated the absence of cytotoxic effects under PN concentrations employed (less than 9.9 μg/mL).

Microscopic observations of cells incubated with these samples revealed that cells presented normal morphology, as cell controls. This result suggests that MNCC may be at Gli concentrations equal or higher than 121 μg/mL. Besides, NRU experiments showed that relative cell viability percentages were over 75 and 100%, independently of irradiation time (Fig. 6). Therefore, CC_{50} value may be at Gli concentrations higher than 121 μg/mL.

From these results, it can be claimed that neither Gli nor its photoproducts accumulated after 45 or 75 min of irradiation presented cytotoxic effect, considering a 15-20% error.

The results presented in this contribution can yield a first approach in the knowledge of the behavior of Andb under an oxidative stress condition. It is known (40) that Gli concentration in serum reach 2-8 μg/mL after 3-4 hours of normal Gli doses of 40-120 mg. The results obtained in cytotoxicity assays could be related to those in blood serum, since the lower Gli concentrations (4.4 and 8.8 μg/mL) experimented are in the range of Gli serum concentrations.

In this paper we have studied the Andb degradation sensitized by Rf, a natural pigment that yield different ROS under photoirradiation, in order to "mimic" the oxidative stress scenery. It is important to notice that there is not accessibly information in bibliography that indicates the exact concentrations of ROS in cells upon oxidative stress. Several techniques allow to indirectly sense

ROS in cells (*in vivo* and *in vitro* experiments), but the exact levels of ROS are still unknown (41-43). Hence, there is not any reference in ROS concentrations through which it could be possible to establish direct relations between the results presented in this paper and oxidative stress in cell. However, if ROS levels are high enough to produce an oxidative stress condition, they accumulate in cells environments where Andb could be present. The important fact under this condition is the possibility that Andb can interact with ROS producing a decrease in their therapeutic action and/or a cytotoxic effect due to products derived from a chemical interaction.

Therefore, considering the importance of oxidative stress highly associated with diabetes type II and the importance that this disease is getting around the worldwide population, the results presented in this paper depict a very important contribution in the knowledge of an aspect that should not be dismissed: the potential interactions between Andb and ROS present in oxidative stress sceneries.

CONCLUSIONS

Our results suggest that Gli and Glip can be degraded in the presence of ROS. Specifically, $O_2(^1\Delta_g)$ participated in the Rf-sensitized photodegradation of both Andb, and also $O_2^{\bullet-}$ in the case of Gli. Besides, Gli showed higher reactivity than Glip against $O_2(^1\Delta_g)$, as was shown in a previous contribution (36).

Through HPLC-mass spectrometry studies, two principal products derived from $O_2(^1\Delta_g)$-mediated degradation of Gli were identified: photoproduct 1 and photoproduct 2. Furthermore, their chemical structures were proposed based on mass spectrometry analysis.

Cytotoxic evaluation in Vero cells demonstrated that neither Gli nor its photoproducts caused cytotoxic effect under the experimental conditions assayed.

Our results provide valuable information for clinical treatment of diabetes type II. In this sense, as Gli or Glip may be exposed to high ROS concentrations (strongly related with oxidative stress scenario in diabetic patients), their potential ROS-mediated degradation would be a critical aspect due to the eventual decrease or loss of their therapeutic action, as well as their potential cytotoxicity.

ROS-mediated degradation of drugs used as a treatment for diseases related to oxidative stress represents a field that deserves special attention. Furthermore, in chronic diseases such as diabetes, in which patients must follow a therapy with medicaments throughout their lives.

AKNOWLEDGEMENTS: This work was supported by Consejo Nacional de Investigaciones Científicas y Técnicas (CONICET) and Secretaría de Ciencia y Técnica de la Universidad Nacional de Río Cuarto (SECyT-UNRC) Argentina. C. Challier thanks CONICET for a PhD fellowship.

TABLES

Table 1. Rate constants for the quenching of ^{1}Rf* by Andb (^1k_q) and rate constants for the ^{3}Rf* quenching by Andb (^3k_q), in buffered solution pH 7.4, 10% methanol.

Compound	**^1k_q x10^{-8} M^{-1} s^{-1}**	**^3k_q x10^{-8} M^{-1} s^{-1}**
Gli	20 ± 2	10 ± 1
Glip	NQ[†]	4.0 ± 0.1

[†]NQ: no quenching observed.

Table 2. Oxygen uptake relative rates, Rf-sensitized, for Gli ($5x10^{-4}$ M) and Gli ($2x10^{-4}$ M) in the absence and in the presence of specific ROS-inhibitors (5.0 mM NaN_3, 1mg/100ml CAT and 1mg/100ml SOD). Solvent: buffered solutions pH 7.4, methanol 10%.

System	v_r
Gli	1.0±0.1
Gli + SOD	1.6±0.1
Gli + CAT	1.1±0.1
Gli + NaN3	0.10±0.01
Glip	1.0±0.1
Glip + SOD	1.0±0.1
Glip + CAT	0.94±0.09
Glip + NaN_3	0.49±0.05

Table 3. Principal results obtained from HPLC-Mass Spectrometry analysis of $O_2(^1\Delta_g)$-mediated photodegradation products of Gli ($5x10^{-4}$ M). Samples were prepared in buffered solutions (pH 7.4, 10% methanol) in the presence of the sensitizer PN ($A_{365nm} = 0.5$), and analyzed without irradiation and after 60 min of irradiation.

Sample	Chromatographic characterization	Molecular ions	Structure proposed
Without irradiation	t_R = 11.9 min	$(M+H)^+$ = 324 uma $(M+K)^+$ = 362 uma	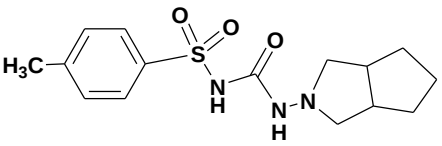 **Gli**
Irradiated 60 min	t_R = 3.9 min	$(M+H)^+$ = 196.3 uma	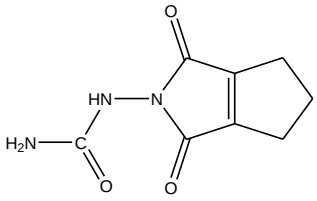 **Photoproduct 1**
	t_R = 13.2 min	$(M+H)^+$ = 388 uma	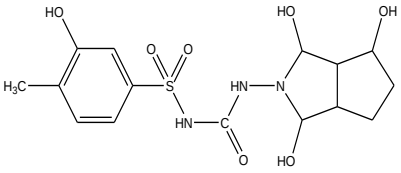 **Photoproduct 2**

SCHEMES AND FIGURE CAPTIONS

Scheme 1. Chemical structures of Gliclazide (Gli) and Glipizide (Glip).

Scheme 2. Possible reaction pathways in the sensitized photoirradiation of Andb. S represents sensitizer (Rf or PN); A, represents a photooxidizable compound (Andb in this paper).

Scheme 3. ROS deactivation pathways in the presence of specific ROS-inhibitors: SOD, CAT, and NaN_3.

Figure 1. Spectral evolution of $1x10^{-4}$ M Gli + 0.02 mM Rf *vs.* 0.02 mM Rf, upon visible-light photoirradiation. **Insert:** Oxygen consumption of **(a)** $5x10^{-4}$ M Gli and **(b)** $2x10^{-4}$ M Glip, under Rf-sensitized irradiation. All the experiments were made in buffered solution pH 7.4, 10% methanol.

Figure 2. Stern-Volmer plots from time-resolved quenching of ^{1}Rf* by **(a)** Gli and **(b)** Glip. **Insert:** Spectral evolution of $1x10^{-4}$ M Glip + 0.02 mM Rf *vs.* 0.02 mM Rf, upon visible-light photoirradiation. Solvent: buffered solution pH 7.4, 10% methanol.

Figure 3. Stern-Volmer plots for the quenching of ^{3}Rf* by (a) Gli and (b) Glip. **Insert:** Spectral evolution of Riboflavin (0.02 mM) upon visible-light- photoirradiation: (a) without additives, unirradiated, (b) without additives, after 7 min of irradiation and (c) in the presence of Gli $5x10^{-4}$ M, after 7 min of irradiation. All the experiments were made in argon-saturated buffered solutions pH 7.4, methanol 10%.

Figure 4. Transient species spectra. **(a)** 0.01 mM Rf obtained 2 μs after the laser pulse in the absence of Andb, and **(b)** 0.01 mM Rf + $5x10^{-4}$ M Gli obtained 20 μs after the laser pulse. **Insert: (a)** 0.01 mM Rf obtained 2 μs after the laser pulse in the absence of Andb, and **(b)** 0.01 mM Rf + $5x10^{-4}$ M Gli obtained 20 μs after the laser pulse, normalized at 670 nm.

Figure 5. Oxygen uptakes of buffered solutions (0.02 mM Rf, pH 7.4 methanol 10%) of $5x10^{-4}$ M Gli, under stationary Rf-sensitized irradiation in the absence **(a)** and in the presence of specific ROS-inhibitors: **(b)** 5.0 mM NaN_3, **(c)** 1 mg/100 ml CAT and **(d)** 1 mg/100 ml SOD.

Figure 6. Relative Cell Viability (RCV) of Vero cells cultures treated with buffered Gli (1617 μg/mL) / PN (< 9.9 μg/mL) solutions (pH 7.4, DMSO less than 1%) without irradiation, and after 45 and 75 min of irradiation. Results are presented as a percentage.

REFERENCES

1. Liu, Y., H. Zhao, H. Li, B. Kalyanaraman, A. C. Nicolosi, D. D. Gutterman. (2003) Mitochondrial sources of H_2O_2 generation play a key role in flow-mediated dilation in human coronary resistance arteries. *Circ. Res.* **93**, 573-580.

2. Guzy, R. D., P.T. Schumacker. (2006) Oxygen sensing by mitochondria at complex III: the paradox of increased reactive oxygen species during hypoxia, *Exp. Physiol.* **91**, 807-819.

3. Dröge, W. (2002) Free radicals in the physiological control of cell function. *Physiol. Rev.* **82**, 47-95.

4. Halliwell, B., O. I. Aruoma. (1991) DNA damage by oxygen-derived species. Its mechanism and measurement in mammalian systems. *FEBS Lett.* **281**, 9-19.

5. Chance, B., H. Sies, A. Boveris. (1979) Hydroperoxide metabolism in mammalian organs. *Physiol. Rev.* **59,** 527-605.

6. Halliwell, B., J.M.C. Gutteridge. (1986) Oxygen free radicals and iron in relation to biology and medicine: some problems and concepts. *Arch. Biochem. Biophys.* **246**, 501-514.

7. Waris, G., H. Ahsan. (2006) Reactive oxygen species: role in the development of cancer and various chronic conditions. *J. Carcinog.* **5**, 14-14. doi: 10.1186/1477-3163-5-14.

8. Rudich, A., A. Tlrosh, R. Potashnik, R. Hemi, H. Kanety, N. Bashan. (1998) Prolonged oxidative stress impairs insulin-induced GLUT4 translocation in 3T3-L1 adipocytes, *Diabetes.* **47**, 1562-1569.

9. Loukogeorgakis, S.P., M.J. Van den Berg, R. Sofat, D. Nitsch, M. Charakida, B. Haiyee. (2010) Role of NADPH oxidase in endothelial ischemia/reperfusion injury in humans. *Circulation.* **121**, 2310-2316.

10. Butterfield, D.A. (1997) Beta-Amyloid-associated free radical oxidative stress and neurotoxicity: implications for Alzheimer's disease. *Chem. Res. Toxico.* **10**, 495-506.

11. American Diabetes Association (2010). Diagnosis and classification of diabetes mellitus. *Diabetes Care.* **33,** S62–S69.

12. Robertson, A.P. (2004) Chronic oxidative stress as a central mechanism for glucose toxicity in pancreatic islet beta cells in diabetes. *J. Biol. Chem.* **279**, 42351-42354.

13. Tiedge, M., S. Lortz, J. Drinkgern, S. Lenzen. (1997) Relation between antioxidant enzyme gene expression and antioxidative defense status of insulin-producing cells. *Diabetes.* **46**, 1733-1742.

14. DeFronzo, R.A. (1999) Pharmacologic therapy for type 2 diabetes mellitus. *Ann. Int. Med.* **131**, 281-303.

15. Sathya, V., V.K. Gopalakrishnan. (2014) In vitro analysis of phytochemicals epicatechin, naringenin, myricetin against Hep3B cell lines and VERO cell lines. *Amer J Drug Disc Devel* **4**, 232-240.

16. Gutleb, A.C., E. Morrison, A.J. Murk. (2002) Cytotoxicity assays for mycotoxins produced by Fusarium strains: a review. *Environ Toxicol Pharmacol* **11**, 309-320.

17. Osada, N., A. Kohara, T. Yamaji, N. Hirayama, F. Kasai, T. Sekizuka, M. Kuroda, K. Hanada. (2014) The genome landscape of the african green monkey kidney-derived Vero cell line. *DNA Res.* **21**(6), 673-683.

18. Bertolotti, S.G., G.A. Arguello, N.A. García. (1991) Effect of the peptide bond on the singlet molecular oxygen mediated photooxidation of tyrosine and tryptophan dipeptides. A kinetic study. *J. Photochem. Photobiol. B: Biol.* **10,** 57-70.

19. Criado, S., N.A. García. (2010) A comparative kinetic and mechanistic study between tetrahydrozoline and naphazoline toward photogenerated reactive oxygen species. *Photochem. Photobiol.* **86**, 23-30.

20. Chacón, J.N., J. McLearie, R.S. Sinclair. (1988) Singlet oxygen yields and radical contributions in the dye-sensitised photo-oxidation in methanol of esters of polyunsaturated fatty acids (oleic, linoleic, linolenic and arachidonic). *Photochem. Photobiol.* **47**, 647-656.

21. Barbieri, Y., W.A. Massad, J.D. Díaz, J. Sanz, F. Amat-Guerri, N.A. García. (2008) Photodegradation of bisphenol A and related compounds under natural-like conditions in the presence of riboflavin: Kinetics, mechanism and photoproducts. *Chemosphere.* **73,** 564–571.

22. Schweitzer, C., R. Schmidt. (2003) Physical mechanisms of generation and deactivation of singlet oxygen. *Chem. Rev.* **103,** 1685–1757.

23. Vanden Berghe, D.A., A.J. Vlietinck (1991) Screening methods for antibacterial and antiviral agents from higher plants. In Methods in Plant Biochemistry (Edited by P.M. Dey, J.D. Harbone). p.p. 47–69, Academic Press, London, England.

24. Rajbhandari, M., U. Wegner, M. Jülich, T. Schöpke, R. Mentel. (2001) Screening of Nepalese medicinal plants for antiviral activity. *J. Ethnopharmacol.* **74**, 251–255.

25. Seth, R., S. Yang, S. Choi, M. Sabean, E.A. Roberts (2004) In vitro assessment of copper-induced toxicity in the human hepatoma line, Hep G2. *Toxicol. In Vitro.* **18**, 501–509.

26. Weber, G., F.W.J. Teale (1957) Determination of the absolute quantum yield of fluorescent solutions. *Trans Faraday Soc.* **53**, 646-655.

27. Encinas, M.V., A.M. Rufs, S. Bertolotti, C.M. Previtali (2001) Free radical polymerization photoinitiated by riboflavin/amines. Effect of the amine structure. *Macromolecules.* **34**, 2845-2847.

28. Bauer, A.W., W.M. Kirby, J.C. Sherris, M. Turk (1966) Antibiotic susceptibility-testing by a standardized single disk method. *Am. J. Clin Pathol.* **45**, 493-496.

29. Heelis, P.F. (1991) The Photochemistry of Flavins. In Chemistry and Biochemistry of Flavoenzymes, Vol. 1. (Edited by F. Muller). p.p. 171-193. CRC Pess, Boca Raton, Florida, EE. UU.

30. Orellana, B., A.M. Rufs, M.V. Encinas, C.M. Previtali, S. Bertolotti. (1999) The photoinitiation mechanism of vinyl polymerization by riboflavin/ triethanolamine in aqueous medium. *Macromolecules.* **32**, 6570-6573.

31. Lu, C., G. Bucher, W. Sander. (2004) Photoinduced interactions between oxidized and reduced lipoic acid and riboflavin (vitamin B2). *Chem. Phys. Chem.* **5**, 47–56.

32. Silva, E., R. Ugarte, A. Andrade, A.M. Edwards. (1994) Riboflavin-sensitized photoprocesses of tryptophan. *J. Photochem. Photobiol. B: Biol.* **23**, 43-48.

33. Wilkinson, F., W. Helman, A.B. Ross. (1995) Rate constants for the decay of the lowest electronically excited singlet state molecular oxygen in solution. An expanded and revised compilation. *J. Phys. Chem. Ref. Data.* **24**, 663–1021.

34. Zang, L.Y., H.P. Misra. (1992) Superoxide radical production during the autoxidation of 1-methyl-4-phenyl-2,3-dihydroxypyridinium perchlorate. *J. Biol. Chem.* **267,** 17547–17552.

35. Frati, E., A.M. Khatib, P. Front, A. Panasyuk, F. Aprile, R.D. Mitrovic. (1997) Degradation of hyaluronic acid by photosensitized riboflavin in vitro. Modulation of the effect by transition metals, radicals quenchers and metal chelators. *Free Radic. Biol. Med.* **22**, 1139–1144.

36. Afanas´ev, I.B. (1989) Superoxide ion: chemistry and biological implications, Vol. 1. CRC Press, Boca Ratón, Florida, EE. UU.

37. Reynoso, E., M.B. Spesia, N.A. García, M.A. Biasutti, S. Criado. (2015) Riboflavin-sensitized photooxidation of Ceftriaxone and Cefotaxime. Kinetic study and effect on *Staphylococcus aureus*. *J. Photochem. Photobiol. B: Biol.* **142**, 35–42.

38. Koizumi, M., S. Kato, N. Mataga, T. Matsuura, I. Isui. (1978). In photosensitized reactions. pp. 218-219. Kagakudogin Publishing Co., Kyoto, Japan.

39. Challier, C., P. Beassoni, C. Boetsch, N.A. García, M.A. Biasutti, S. Criado. (2015) Interaction between Human Serum Albumin and antidiabetic compounds and its influence on the $O_2(^1\Delta_g)$-mediated degradation of the protein. *J. of Photochem. Photobiol. B: Biology.* **142**, 20-28.

40. Palmer, K.J, R.N. Brogden. Gliclazide (1993). An Update of its Pharmacological Properties and Therapeutic Efficacy in Non-Insulin-Dependent Diabetes Mellitus. *Drugs*, **46** (1), 92-125.

41. Lushchak, VI. (2014). Free radicals, reactive oxygen species, oxidative stress and its classification. *Chem Biol Interact.* **224**, 164-75.

42 Finkel, T., N. J. Holbrook. (2000). Oxidants, oxidative stress and the biology of ageing. *Nature*. **4**, 239-247.

43 Sies, H. (2018). On the history of oxidative stress: Concept and some aspects of current development. *Curr. Opin. Toxicol*. **7**,122–126.